28. Couttlet, P. *et al.* Messenger RNA deadenylation precedes decapping in mammalian cells. *Proc. Natl Acad. Sci. USA* **94,** 5628–5633 (1997).
29. Flavell, S. W. *et al.* Genome-wide analysis of MEF2 transcriptional program reveals synaptic target genes and neuronal activity-dependent polyadenylation site selection. *Neuron* **60,** 1022–1038 (2008).
30. Kharchenko, P. V., Tolstorukov, M. Y. & Park, P. J. Design and analysis of ChIP-seq experiments for DNA-binding proteins. *Nature Biotechnol.* **26,** 1351–1359 (2008).
31. Rozowsky, J. *et al.* PeakSeq enables systematic scoring of ChIP-seq experiments relative to controls. *Nature Biotechnol.* **27,** 66–75 (2009).
32. Robertson, A. G. *et al.* Genome-wide relationship between histone H3 lysine 4 mono- and tri-methylation and transcription factor binding. *Genome Res.* **18,** 1906–1917 (2008).
33. Skellam, J. G. The frequency distribution of the difference between two Poisson variates belonging to different populations. *J. R. Stat. Soc. A* **109,** 296 (1946).
34. Efron, B. Microarrays, empirical Bayes and the two-groups model. *Stat. Sci.* **23,** 1–22 (2008).
35. Benjamini, Y. & Hochberg, Y. Controlling the false discovery rate: a practical and powerful approach to multiple testing. *J. Roy. Statist. Soc. Ser. B. Methodol.* **57,** 289–300 (1995).
36. Jothi, R., Cuddapah, S., Barski, A., Cui, K. & Zhao, K. Genome-wide identification of *in vivo* protein–DNA binding sites from ChIP-Seq data. *Nucleic Acids Res.* **36,** 5221–5231 (2008).
37. Ooe, N. *et al.* Identification of a novel basic helix-loop-helix-PAS factor, NXF, reveals a Sim2 competitive, positive regulatory role in dendritic-cytoskeleton modulator drebrin gene expression. *Mol. Cell. Biol.* **24,** 608–616 (2004).
38. Lin, Y. *et al.* Activity-dependent regulation of inhibitory synapse development by Npas4. *Nature* **455,** 1198–1204 (2008).
39. Huang, D. W., Sherman, B. T. & Lempicki, R. A. Systematic and integrative analysis of large gene lists using DAVID Bioinformatics Resources. *Nature Protocols* **4,** 44–57 (2009).
40. Dennis, G. Jr *et al.* DAVID: Database for Annotation, Visualization, and Integrated Discovery. *Genome Biol.* **4,** 3 (2003).

神経疾患と細胞骨格

竹本-木村さやか*　上田（石原）奈津実*　布施俊光*　上條諭志*　尾藤晴彦*

神経回路網の発達期には，幼弱神経細胞の移動，軸索・樹状突起の形成・伸展がまず起こる．このような神経細胞の形態形成過程ではアクチンや微小管などの細胞骨格系の貢献が大である．さらに，伸展した軸索が投射先の樹状突起と遭遇し，シナプスが形成・成熟する際にも，非常に動的な細胞形態制御が不可欠となる．最近では，成熟回路におけるシナプス機能についても，絶えず再編成しつづけ，動的に維持されていることが明らかとなっている．このようなダイナミックな神経細胞骨格制御がいったん破綻すると，どのような疾患が起こるのか．本稿では細胞骨格機能障害が引き起こす分子病態と最終的な脳高次機能異常について概説する．

はじめに

近年，ヒト遺伝性脳高次機能異常の家系研究から，種々の原因候補遺伝子が単離同定されてきた．興味深いことに，原因遺伝子の多くは，脳発達の途上で神経回路形成を制御すると考えられる細胞骨格制御因子である．神経回路網の発達期には，初期の細胞移動から，後期のシナプス形成期にいたるまで，数多くの神経細胞形態形成制御過程が存在する．さらに，神経回路の成熟後も，シナプス機能が機能的・形態的に維持され，再編成しつづけることが最近の知見により明らかとなっている．このように考えると，アクチン・微小管などの細胞骨格機能の遺伝的障害が，脳高次機能異常に結びついていることは偶然ではなく，必然であるとすらいえよう．本稿では，これまでに明らかになっている神経細胞骨格の制御メカニズムとその意義について簡潔に紹介し，さらに，いくつかの具体的な疾患について，その細胞骨格機能障害が引き起こす分子病態と最終的な脳高次機能異常について概説する．

Key Words
アクチン
微小管
シナプス
レセプタートラフィッキング
Rho

1．神経回路発達における細胞骨格制御の意義

20世紀初頭に，Ramón y Cajalはニューロン・ドクトリンという仮説を著し，そのなかで，脳神経系が数多くの神経細胞種から成り，これら多数の細胞が融合せず，複雑な接合（すなわちシナプス）を互いに形成することにより，その複雑な脳機能を果たしている可能性を明らかにした[1]．この考えは，筋肉という興奮性組織が，むしろ筋細胞融合によって協調的収縮という機能を獲得するのとは，まったく様相を異にするということを喝破した点で画期的であった．

* TAKEMOTO－KIMURA Sayaka, AGETA－ISHIHARA Natsumi, FUSE Toshimitsu, KAMIJO Satoshi, BITO Haruhiko/東京大学大学院医学系研究科　神経生化学教室

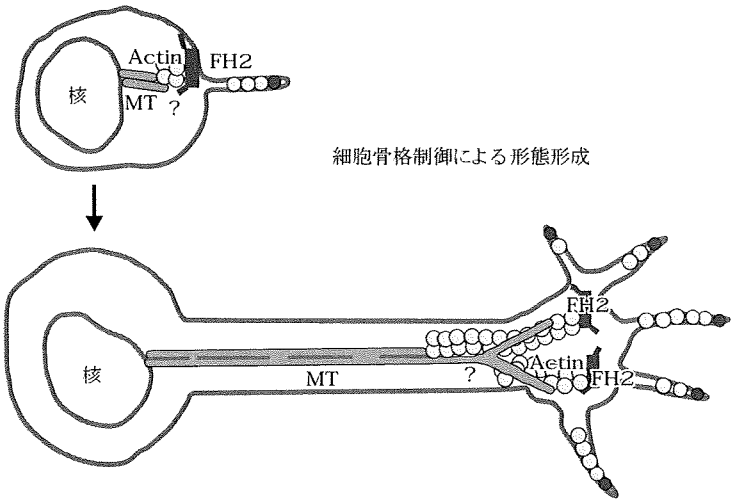

図　微小管 MT)とアクチン細胞骨格 Actin)の相互作用による神経細胞の形態形成制御 Bito H, 2003[18]より改変引用)
両骨格の協調には，フォルミンタンパク質 FH2)などが関与していると考えられている．

それから 100 年以上が過ぎ，シナプスという神経回路接合部分の形成と機能構築に関する知見は飛躍的に進展した．脳神経系の発達の途上では，①終末分化終了後に，細胞種特異的な転写因子群の発現制御により，興奮性・抑制性などの神経細胞の分化が規定され，つづいて，②主として微小管制御にもとづいた細胞移動に依拠した脳領野ならびに大脳皮質層構造の構築が進み，③細胞極性の成立と同時に，軸索ならびに樹状突起とよばれる 2 種類の機能的に分化した突起を伸ばし，軸索先端部が標的となる神経細胞の樹状突起へ目掛けて投射する．このような 3 つの過程が，シナプス形成に先立つ神経回路形成の根幹をなすと考えられている[2]．

そして最終的には，軸索の先端の神経終末には，神経伝達物質放出を司る分子装置が整備され，樹状突起スパイン上の後シナプス肥厚部 post synaptic density: PSD)とよばれる特殊な構造と対をなし，細胞間接着装置であるシナプスを形成する．こうして神経伝達物質の放出と受容を介して情報を一方向的に伝達する機構が完成する[2]．

このように，神経細胞の移動，軸索および樹状突起の形成・伸展や，シナプス形成過程には，アクチン・微小管細胞骨格による動的制御が不可欠と考えられている（図）[18]．

2．成熟神経回路の形成後の動的細胞骨格の役割

一方，成熟神経回路形成が完了した後は，神経細胞の形態やシナプス結合は大きく変化せず，細胞骨格系は静的な構造支持装置であるという考えが長らく主流であった．しかしながらたとえば Donald O Hebb は，シナプス可塑性を予言する考察のなかで，シナプスの増減を説明しうる機構として活動依存的な突起の動的な新生・消退を予見した[3]．長期増強や長期抑圧などのシナプス可塑性の実在が確認された 1980 年以降，実際にシナプスを含む神経形態の活動依存的変化を実証することが急務となった．興奮性シナプスの多くは，スパインとよばれる樹状突起上の微小な突起に形成されているが，最近シナプス伝達の長期増強 long term potentiation: LTP)に伴いスパイン，スパイン頸部，スパイン数などが変化する様相がついに明らかにされた[4]．このような過程においては，シナプス維持とスパイン形態制御とその協調性がきわめて重要であり，シナプス後部の分子構築が，動的なアクチン骨格と PSD 分子間の相互作用により，規定されていることが示されている[5][6]．

3．脳発達期における神経細胞骨格制御の破綻がもたらす脳機能異常

近年，ヒトにおける遺伝性の脳高次機能異常（精神遅滞，特異的認知障害など）や精神疾患の家系研究から，さまざまな原因候補遺伝子が同定されるようになった．すると驚くべきことに，これらの原因遺伝子のうちの少なからずが，神経細胞骨格制御にとって重要と考えられる分子をコードする例が次々と報告された．

たとえば脳のしわが欠失する広範な脳病変を伴う滑脳症は，胎生期の脳発達における細胞移動の異常を基礎病変としている遺伝性疾患である．その原因遺伝子は近年LIS1やdoublecortinといった微小管結合タンパク質であることが明らかになり，機能的神経回路形成初期における微小管制御の重要性が改めて証明された．さらに，統合失調症家系の解析から注目されている*DISC-1*遺伝子産物が，これら微小管結合タンパクと分子複合体を形成することから，脳発生における神経細胞の移動不全が精神疾患発症に結びつく可能性が示唆されてきている[7]．

この後の神経回路形成最終段階では，軸索末端と樹状突起のあいだでシナプスが形成される．このとき，シナプス前膜とシナプス後膜のあいだでは，細胞接着分子を介した積極的な会合が形成されると考えられている．Neurexin/Neuroligin複合体や，これとシナプス後部において結合するShank 3の変異を伴う家族性自閉症の存在が明らかになり，Shankはcortactinを介してシナプス後部のアクチン骨格と結合していることから，形成されたシナプスの数や位置の制御破綻が，自閉症発症の一因となっているのかもしれない．

一方，古くから，精神遅滞とシナプスが局在している構造であるスパインの形態の異常の関係を示唆する病理所見の報告が知られていた．しかしその因果関係がもっとも最初に明らかになったのは，伴性遺伝性精神遅滞と低分子量Gタンパク質制御の関係の研究を通じてである．伴性遺伝性精神遅滞の候補原因遺伝子としてRhoGAP（GTPase activating protein）分子であるoligophrenin-1，Cdc42/Racの下流のエフェクターであるPak3（p21-activated kinase3），RhoGEF（guanine nucleotide exchange factor）であるARHGEF6などが同定された[8]が，実際これら遺伝子を改変したマウスにおいて，脳発達期におけるスパイン形態の異変が顕著に認められた[9][10]．さらに，外界からの多様な感覚入力を担う神経回路の形成と成熟には，神経突起のダイナミックな進展退縮が必要であり，アクチン重合制御やアクトミオシン系による物質輸送制御が不可欠と考えられている．たとえば，知覚回路の異常の例としては，無症候性遺伝性難聴DFNA1があげられる．この原因遺伝子としてRhoエフェクターのmDia1が同定されている[11]．同様に，Williams症候群は，多くの発達段階にかかわる遺伝子群の欠失により生じるが，とくに*LIMK1*遺伝子の欠損を含む患者では，視空間形成認知機能の特異的な障害が生じる．LIMK1は，Rho結合キナーゼROCKの基質であり，スパインや軸索先端の成長円錐におけるアクチン重合を制御していると考えられている．実際に，LIMK1ノックアウトマウスにおいては，樹状突起形成異常と神経可塑性異常などが報告されている[12]．

このような知見から，神経回路網がマクロ的にもミクロ的にも正確に形成される過程に関与する多くの分子の破綻により，脳高次機能異常が引き起こされることが明らかとなり，脳発達期における正確な細胞骨格制御の重要性が裏付けられた．

4．成熟神経回路における細胞骨格制御破綻のもたらす病態

では，微小管あるいはアクチンからなる神経細胞骨格の機能異常が，成熟脳にて発生した場合は，何が起こるのであろうか．もっとも顕著な例として，アルツハイマー病があげられる．この病変の本質が神経原線維変化における過剰リン酸化tauの蓄積であるという発見以来，神経細胞の病態・代謝異常の最終結末として，重篤な細胞骨格障害をきたし，結果として神経変性や脳機能異常が生じると考えられた．

さらに，アルツハイマー病発症初期のベータアミロイド蓄積においても，アクチン細胞骨格の関与が想定されている．たとえば，LIMKによるcofilinリン酸化が増強され，その結果神経変性が増悪する発端となる可能性が報告されている[13]．ほぼ同様の機構により，アクチン重合制御因子profilinのROCKによるリン酸化により，

ハンチントン病原因遺伝子産物huntingtinの細胞内凝集体形成が促進される可能性も示唆されている[14]．すなわち，成熟神経回路における正常な神経細胞骨格の役割の一つは，タンパク質の流通・品質管理を通じて，異常なタンパク凝集体形成を未然に防ぐことであるといえる．このことに合致して，前述したRhoGAP分子oligophrenin-1変異の研究から，Rhoシグナリングが破綻すると，シナプス前ならびにシナプス後機能の両者において，小胞輸送やレセプタートラフィッキングに顕著な異常が現れることが判明している[15)~17)]．すなわち，低分子量Gタンパク質を介したアクチン細胞骨格動態制御によって，成熟神経回路のシナプス伝達・シナプス可塑性の発現が刻一刻と決定されている可能性が強く示唆されている．

5．神経疾患における細胞骨格動態への薬理学的介入による機能回復の試み

このように，細胞骨格系の機能破綻により，多くの脳高次機能異常，さらには神経・精神疾患の発症が引き起こされる可能性が高い．では，このような細胞骨格動態の異常を薬理学的に回復する戦略は不可能なのであろうか．いったん発達期に起きてしまった回路形成異常を元に回復することは困難であることが予測されるが，成体脳における情報伝達異常については，薬理学的回復の可能性がある．もしそうであれば，これにより，病態が果たしてどのように改善するか，大いに期待される．

実際，アルツハイマー病のアミロイド沈着やポリグルタミン凝集体の形成がROCK阻害薬により改善するという報告が数年前から発表されてきている[14]．また，現時点ではあくまでも遺伝子改変マウスレベルでの知見に留まっているが，oligophrenin欠損マウスにおけるRhoシグナル活性化に伴うシナプス伝達・可塑性異常は，成体でもRhoシグナル伝達系の抑制により回復することが明らかとなっている[17]．このように，いまだ断片的な実験事実によってしか支持されていないが，細胞骨格制御破綻によってもたらされる神経疾患の少なくとも一部については，ROCK阻害薬などの薬剤の効果の検証が待たれるところである．

一方，神経回路網形成の初期には，神経細胞におけるRho/ROCK/mDia1シグナル伝達系が突起形成・伸展の制御に関与している[18]．このことは，脊髄損傷などによる後天的な突起発達障害のケースにおいて，Rhoシグナルの人為的修飾により，神経突起再生を誘導・制御するという新たなアプローチの可能性を示唆するものである．事実，そのような試みはすでに米国・カナダでは実際に始まりつつある．McKerracherらは，MAGやNogo-66など神経損傷後の軸索再生を抑制する諸因子がp75NGFRを介して，脊髄損傷後に脊髄における低分子量GタンパクRho活性が持続的に上昇することを見出した．そしてマウス胸髄損傷モデルを用い，脊髄切断後早期にRho活性やROCK活性を遮断することにより，軸索再生スピードの有意な加速や，運動能の著しい回復を得ることに成功している[19]．ラット胸髄切断モデルを用いたStrittmatterらも，ROCKインヒビター投与時には，同様に神経線維再生・運動能回復がともに促進されることを追認していることは特筆に値する[20]．

これらの報告から大胆に考察してみると，Rho/ROCK情報伝達系は，ほかの低分子量Gタンパク質経路と協調的あるいは拮抗的に連携しながら，アクチン細胞骨格制御を介し，単に形態制御をおこなうのみでなく，神経細胞内の種々のタンパクの輸送・集積・品質管理・分解に対しても何らかの恒常的制御を及ぼしているのかも知れない（図　）．このような観点からもROCKインヒビターの神経疾患に対する創薬標的としての新たな可能性について，今後検証することが急務と考えられる．

おわりに

発育時における脳神経回路網の発達異常が，精神・認知・神経の障害をもたらす原因の一つであるという考え方が最近有力視されている．またいったん正常な発育を遂げた場合でも，正常範囲の加齢とともに，脳神経回路網の機能的異常が蓄積し，脳高次機能（意識，情動，記憶，意欲，注意など）の機能障害が高い確率で襲ってくるといわれている．今日までに得られた知見により，脳神経系における細胞骨格制御が新たな分子治療のための創薬標的となりつつあり，神経回路網損傷や神経変性による脳高次機能低下から回復する，という可能性が実現可能なレベルまで徐々に到達しつつあることを，本稿で

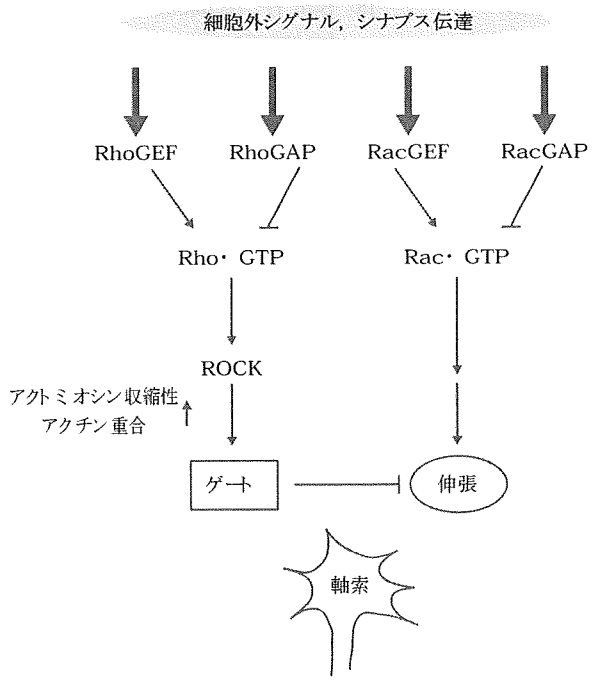

図　神経細胞骨格の作用点に対する２重制御の原理：突起伸張の例 筆者作成）
突起伸張 axon growth）に対しては，２つの低分子量Gタンパク Rac と Rho が拮抗的に２重制御をかけているため，たとえば Rac による正の制御の低下を，Rho による負の制御の抑制により代償することが可能となる．ROCK 阻害薬は，Rho 下流の多くの ROCK 作用点に対して効果をもつ．小胞輸送，レセプタートラフィッキングにおいても同様の２重制御機構の存在が想定されているがその分子的実体はまだ不明である．

は紹介した．今後の神経細胞骨格シグナル伝達の理解が深まれば，精神遅滞や精神疾患の動物モデルにおいても，シナプス形成・維持やスパイン形態の操作・修復までが制御可能となると信じ，期待して止まない次第である．

文　献

1) Cajal SR: *Textura del sistema nervioso del hombre y de los vertebrados*（Textbook on the nervous system of man and the vertebrates）, 2002, pp.1897−1899
2) Principles of Neural Science, Fourth Edition. ed by Kandel ER *et al*, McGraw−Hill, New York, 2000
3) Hebb DO: The Organization of Behavior: A Neuropsychological Theory, Wiley 1949.
4) Matsuzaki M *et al*: Structural basis of long−term potentiation in single dendritic spines. *Nature* 429: 761−766, 2004
5) Kuriu T *et al*: Differential control of postsynaptic density scaffolds via actin−dependent and−independent mechanisms. *J Neurosci* 26: 7693−7706, 2006
6) Nonaka M *et al*: Essential contribution of the ligand−binding beta B/beta C loop of PDZ1 and PDZ2 in the regulation of postsynaptic clustering, scaffolding, and localization of postsynaptic density−95. *J Neurosci* 26: 763−774, 2006
7) Olson EC *et al*: Smooth, rough and upside−down neocortical development. *Curr Opin Genet Dev* 12: 320−327, 2002
8) Chechlacz M *et al*: Is mental retardation a defect of synapse structure and function? *Pediatr Neurol* 29: 11−17, 2003
9) Khelfaoui M *et al*: Loss of X−linked mental retardation gene oligophrenin 1 in mice impairs spatial memory and leads to ventricular enlargement and dendritic

spine immaturity. *J Neurosci* 27: 9439–9450, 2007
10) Hayashi ML *et al*: Altered cortical synaptic morphology and impaired memory consolidation in forebrain-pecific dominant-negative PAK transgenic mice. *Neuron* 42: 773–787, 2004
11) Lynch ED *et al*: Nonsyndromic deafness DFNA1 associated with mutation of a human homolog of the Drosophila gene diaphanous. *Science* 278: 1315–1318, 1997
12) Meng Y *et al*: Abnormal spine morphology and enhanced LTP in LIMK-1 knockout mice. *Neuron* 35: 121–133, 2002
13) Heredia L *et al*: Phosphorylation of actin-depolymerizing factor/cofilin by LIM-kinase mediates amyloid beta-induced degeneration: a potential mechanism of neuronal dystrophy in Alzheimer's disease. *J Neurosci* 26: 6533–6542, 2006
14) Shao J *et al*: Phosphorylation of profilin by ROCK1 regulates polyglutamine aggregation. *Mol Cell Biol* 28: 5196–5208, 2008
15) Nakano-Kobayashi A et al: The Rho-linked mental retardation protein OPHN1 controls synaptic vesicle endocytosis via endophilin A1. *Curr Biol* 19: 1–7, 2009
16) Kasri NN *et al*: The Rho-linked mental retardation protein oligpphrenin-1 controls synapse maturation and plasticity by stabilizing AMPA receptors. *Genes Dev* 23: 1289–1302, 2009
17) Khelfaoui M *et al*: Inhibition of RhoA pathway rescues the endocytosis defects in oligophrenin1 mouse model of mental retardation. *Hum Mol Genet* 18: 2575–2583, 2009
18) Bito H: Dynamic control of neuronal morphogenesis by rho signaling. *J Biochem* 134: 315–319, 2003
19) Dergham P *et al*: Rho signaling pathway targeted to promote spinal cord repair. *J Neurosci* 22: 6570–6577, 2002
20) Fournier AE *et al*: Rho kinase inhibition enhances axonal regeneration in the injured CNS. *J Neurosci* 23: 1416–1423, 2003

BITO Haruhiko

びとう・はるひこ
1990年，東京大学医学部卒業
1993年，同大学院修了(博士)医学，授与)
1993～97年，スタンフォード大学大学院医学研究科常勤研究員
1997年，京都大学大学院医学研究科助手
1998年，同講師
2003年，東京大学大学院医学系研究科助教授
2007年，同准教授 現職)
専門は，神経生化学
趣味は，読書，音楽鑑賞

TAKEMOTO-KIMURA Sayaka

たけもと-きむら・さやか
1999年，名古屋大学医学部卒業
1999年，同大学医学部付属病院医員 研修医)
2000～03年，京都大学大学院医学研究科大学院生
2003年，同大学院博士課程修了 京都大学博士 医学)学位取得)
2003年，東京大学大学院医学系研究科神経生化学助手
2007年，同助教 現職)
専門は，神経生化学，とくに神経回路形成と可塑性の分子機構
趣味は，子供との東大散策

Available online at www.sciencedirect.com
ScienceDirect
Mitochondrion 7 (2007) 125–132
Mitochondrion
www.elsevier.com/locate/mito

Mitochondria and apicoplast of *Plasmodium falciparum*: Behaviour on subcellular fractionation and the implication

Tamaki Kobayashi [a], Shigeharu Sato [b], Shinzaburo Takamiya [c], Kanako Komaki-Yasuda [d], Kazuhiko Yano [d], Ayami Hirata [e], Izumi Onitsuka [e], Masayuki Hata [a], Fumika Mi-ichi [a], Takeshi Tanaka [a], Toshiharu Hase [f], Atsushi Miyajima [e], Shin-ichiro Kawazu [d], Yoh-ichi Watanabe [a], Kiyoshi Kita [a,*]

[a] *Department of Biomedical Chemistry, Graduate School of Medicine, The University of Tokyo, 7-3-1 Hongo, Buinkyo-ku, Tokyo 113-0033, Japan*
[b] *Division of Parasitology, National Institute for Medical Research, The Ridgeway, Mill Hill, London NW7 1AA, UK*
[c] *Department of Molecular and Cellular Parasitology, Juntendo University School of Medicine, 2-1-1 Hongo, Bunkyo-ku, Tokyo 113-8421, Japan*
[d] *Research Institute, International Medical Center of Japan, 1-21-1 Toyama, Shinjuku-ku, Tokyo 162-8655, Japan*
[e] *Laboratory of Cell Growth and Differentiation, Institute of Molecular and Cellular Biosciences, The University of Tokyo, 1-1-1 Yayoi, Bunkyo-ku, Tokyo 113-0032, Japan*
[f] *Division of Enzymology, Institute for Protein Research, Osaka University, 3-2 Yamadaoka, Suita, Osaka 565-0871, Japan*

Received 19 April 2006; accepted 21 September 2006
Available online 9 December 2006

Abstract

The mitochondrion and the apicoplast of the malaria parasite, *Plasmodium* spp. is microscopically observed in a close proximity to each other. In this study, we tested the suitability of two different separation techniques – Percoll density gradient centrifugation and fluorescence-activated organelle sorting – for improving the purity of mitochondria isolated from the crude organelle preparation of *Plasmodium falciparum*. To our surprise, the apicoplast was inseparable from the plasmodial mitochondrion by each method. This implies these two plasmodial organelles are bound each other. This is the first experimental evidence of a physical binding between the two organelles in *Plasmodium*.

Keywords: *Plasmodium falciparum*; Mitochondrion; Apicoplast; Fluorescence-activated organelle fractionation

1. Introduction

Malaria, by far the most important tropical parasitic disease, is caused by a group of parasites *Plasmodium* spp. belonging to the phylum Apicomplexa. Currently, various anti-malarial drug resistant parasite strains are reported and there is a long way for the development of vaccine. Emergence of insecticide resistant mosquito vector limits the current control schemes as well (Greenwood et al., 2005). In order to control this world problem, studies seeking for unique properties of the parasite are indispensable.

Previous study reported malaria parasites obtain most of their energy from glycolysis, if not all (Roth et al., 1988) and malaria parasite possesses one mitochondrion with various shapes at different stages of the intra-erythrocytic development and it is acristae (Slomianny and Prensier, 1986). Mitochondria of *Plasmodium* species carries 6-kb genome, which is the smallest mitochondrial genome ever been reported and encoding only 3 open reading frames with homology to classical mitochondrial protein, cytochrome *c* oxidase subunit I, cytochrome *c* oxidase subunit III and cytochrome *b*, as well as abbreviated rRNA genes (Vaidya et al., 1989; Feagin, 1992). Thus this

Abbreviations: DHOD, dihydroorotate dehydrogenase; FOS, fluorescence-activated organelle sorting; RBC, red blood cell.

* Corresponding author. Tel.: +81 3 5841 3526; fax: +81 3 5841 3444.
E-mail address: kitak@m.u-tokyo.ac.jp (K. Kita).

1567-7249/$ - see front matter © 2006 Elsevier B.V. and Mitochondria Research Society. All rights reserved.
doi:10.1016/j.mito.2006.11.021

organelle heavily depends on most of the proteins and all tRNAs supplied from the outside.

Biochemical analysis suggested that *Plasmodium falciparum* might lack TCA cycle in the erythrocytic stage (see the review by Sherman, 1979). Recent completion of malaria genome project has revealed that the genes necessary for a complete TCA cycle were present in *P. falciparum* (Gardner et al., 2002). However, it still remains unclear whether the TCA cycle is responsible for the further oxidation of glycolysis product. Nevertheless, the activity of the electron transport chain and the membrane potential of this organelle are indispensable for the survival of the parasite. For example, dihydroorotate dehydrogenase (DHOD) involved in the parasite's *de novo* biosynthesis of pyrimidine requires the functional electron transport chain on the mitochondrial membrane as the electron disposal sink (Gutteridge and Trigg, 1970; Gero et al., 1984; Prapunwattana et al., 1988). More recent study showed that the membrane potential of mitochondria formed by respiration is essential for parasite growth (Srivastava et al., 1999) and complex III (ubiquinol-cytochrome *c* reductase) inhibitor, atovaqone, an anti-malarial that is currently in use is reported to disrupt mitochondrial membrane potential resulting in parasite growth reduction (Srivastava et al., 1997).

Aikawa (1966) carried out an extensive morphological study by electron microscope and found a distinctive organelle in the cell of the malaria parasite. This organelle is multi-membrane bound, always observed adjacent to the mitochondrion (see the review by Bannister et al., 2000). Later, a non-mitochondrial extra-chromosomal DNA encoding a set of genes characteristic of the plastid genome was found in apicomplexan parasites including *Plasmodium* spp. *Toxoplasma gondii* and *Theileria* spp. (Wilson et al., 1996; Kohler et al., 1997) localized the plastid genome-like DNA to the multi-membrane organelle in *T. gondii* by *in situ* hybridization, revealing that the distinctive multi-membrane organelle is the plastid of the apicomplexan parasite. The apicomplexan plastid, which is non-photosynthetic, is often called "the apicoplast" for abbreviation. The genome of the apicoplast is one of the smallest known plastid genomes (Wilson et al., 1996; Gardner et al., 2005). The apicoplast depends heavily on proteins imported post-translationally from the cytosol (see the review by Ralph et al., 2004), as does the mitochondrion.

For biochemical studies of each organelle of *Plasmodium* spp., it is necessary to obtain the pure sample. Fry and Beesley (1991) reported a method to prepare the mitochondria from *Plasmodium* spp. by Percoll density gradient centrifugation. Takashima et al. (2001) reported another preparation method using nitrogen cavitation. The mitochondrial preparation by the latter method exhibited a significantly higher succinate dehydrogenase activity than that by the former method (Takashima et al., 2001). By contrast, no method for preparing the plasmodial apicoplast with a significant purity has been reported.

In this study, we combined nitrogen cavitation method with two different fractionation methods, Percoll density gradient centrifugation or fluorescence-activated organelle sorting (FOS), to prepare the mitochondrion of higher purity from *P. falciparum*. Surprisingly, we found that the mitochondrion and the apicoplast were recovered in the same fraction by each fractionation methods, most likely because the two organelles are bound each other. To our knowledge, this is the first report that suggests the presence of a physical connection between the mitochondrion and the apicoplast of *P. falciparum*.

2. Materials and methods

2.1. Parasite cultivation and handling

Plasmodium falciparum (Honduras-1 strain and 3D7 strain) was cultured following the method reported by Trager and Jensen (1976) with modifications. The culture was maintained with 3% hematocrit type A human red blood cell (RBC) in RPMI 1640 medium (Invitrogen) supplemented with 10% (v/v) type A human serum. Prior to the preparation of crude mitochondrial fraction, parasites were synchronised by 5% (w/v) sorbitol as it was described previously (Lambros and Vanderberg, 1979).

2.2. Preparation of the crude P. falciparum mitochondria fraction

Plasmodium falciparum-infected RBC were collected by centrifugation at 800*g* for 10 min at 4 °C (LX-120, TOMY) when parasitemia is more than 5% but not exceeding 10%. Parasite was mainly trophozoite stage as it was confirmed by observing the Giemsa's stained smear. Trophozoite stage was considered because DHOD-specific activity is the highest (F. Mi-ichi, Personal communication). The crude *P. falciparum* were disrupted by nitrogen cavitation as described (Takashima et al., 2001). The pellet obtained after the centrifugation at 23,000*g* for 20 min at 4 °C (Himac CR22, HITACHI) was suspended in 200–400 μl MSE buffer (225 mM mannitol, 75 mM sucrose, 0.1 mM EDTA (Dojin), 3 mM Tris–HCl; pH 7.4) and characterized as a crude mitochondrial fraction (Fig. 1).

2.3. Subcellular fractionation of P. falciparum mitochondria with the Percoll density gradient centrifugation

The crude mitochondrial fraction prepared from *P. falciparum* Honduras-1 strain (1.5 mg protein) was brought to a total volume of 8 ml in 23% (v/v) Percoll (GE Healthcare) in MSE. Percoll sample was centrifuged at 100,000*g* for 1 h at 4 °C (Himac SCP70H, HITACHI, rotor No. RP40). Together with the mitochondrial fraction, beads marker provided by the manufacture was centrifuged in parallel to confirm the formation of gradient and density of each fraction. The gradient was fractionated from top to bottom with glass Pasteur pipette (400 μl/ fraction). The formation

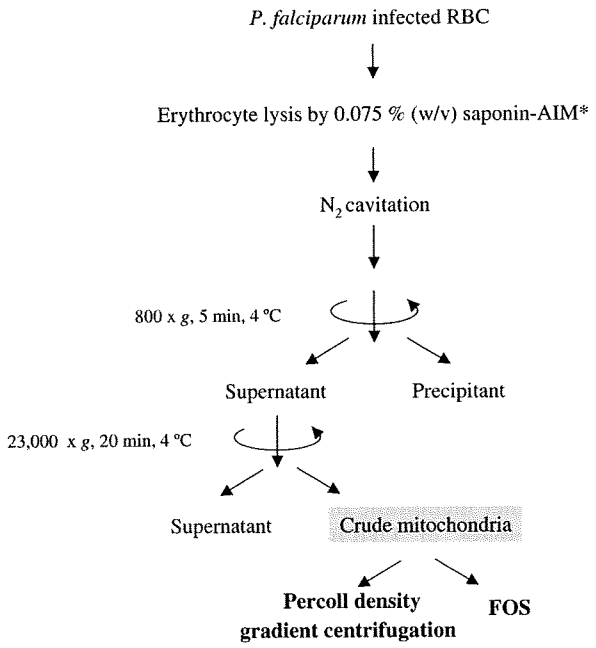

Fig. 1. Crude mitochondria preparation from *P. falciparum* *AIM (120 mM KCl, 20 mM NaCl, 10 mM Pipes, 1 mM $MgCl_2$, 5 mM glucose; pH 6.7).

of the gradient can be affected by factors such as the angle of the rotor. Therefore, it is critical to monitor the formation of the desired gradient by using the density marker beads all the time when one uses different centrifuge and rotor.

DHOD activity was measured to determine the fraction containing mitochondria (Mi-Ichi et al., 2005). DHOD assay was performed at 25 °C using UV3000 spectrophotometer (SHIMADZU) with 1 ml of the reaction mixture containing 45 μM 2,6-dichlorophenolindophenol (DCIP) (Sigma), 100 μM ubiquinone-2 (Sigma) and 2 mM KCN in 30 mM Tris–HCl (pH 8.0). The reaction was initiated by adding 500 μM dihydroorotate and the production of reduced DCIP was monitored at 600 nm (ε=21 mM^{-1} cm^{-1}).

2.4. Protein assay

Protein concentration of *P. falciparum* sample was determined by Bradford method (Bradford, 1976) using Bio-Rad protein assay reagent according to the manual provided by the manufacturer, with bovine serum albumin (PIERCE) as a standard. For the sample that contains Percoll, Percoll was precipitated under the presence of 250 mM NaOH and 0.025% (w/v) Triton X-100 as it was reported (Vincent and Nadeau, 1983) prior to the protein assay.

2.5. Western blot analysis

As Percoll interferes with SDS–PAGE, the fraction of interest was diluted with MSE buffer up to 8.5 ml and centrifuged at 220,000*g* for 1 h at 4 °C (CP10α, 70H, HITACHI) to remove Percoll. Samples were collected as floating pellet and suspended in MSE up to 1.5 ml. Suspended pellet was transferred to 1.5 ml tube and centrifuged at 20,000*g* for 10 minutes at 4 °C (TOMY MX-160). The pellet was re-suspended in MSE buffer. Prepared samples were then run on 12.5% polyacrylamide gel and transferred to nitrocellulose membrane. Membranes were blocked with 5% (w/v) non-fat skim milk powder in 0.5% (v/v) Tween–Tris-buffered saline and afterwards probed with polyclonal antibodies specific to mitochondrion or apicoplast. For the detection of mitochondrion and apicoplast, serum against recombinant *P. falciparum* iron–sulfur cluster subunit of complex II (rPfIp) and ferredoxin (rPfFd) were raised in mouse and rabbit, respectively. The dilution for the first antibody was 1:2000 for anti-rPfIp serum and 1:1000 for anti-rPfFd serum.

2.6. Electron microscopic observation of the subcellular-fractionated sample by the Percoll density gradient centrifugation

Percoll was removed from the sample as described above. Obtained pellet was suspended in fixative solution containing 2% (v/v) glutaraldehyde in 20 mM sodium phosphate buffer (pH 6.8): MSE buffer = 1:1. The sample was fixed overnight at 4 °C and subsequently washed with 20 mM Sodium phosphate buffer (pH 6.8): MSE buffer = 1:1 for three times. The fixed sample was then dehydrated and embedded in resin. Serial sections were cut and observed by transmission electron microscope (HITACHI H-7100).

2.7. GFP fusion constructs and P. falciparum transfection

The expression vector, pSSPF2/PfHSP60-GFP (Sato et al., 2003) was transfected to *Escherichia coli* DH5α and the transfected *E. coli* was grown in the terrific broth. Plasmids were collected by centrifugation and was purified using Plasmid Maxi Kit (Qiagen). The plasmid was verified with restriction digestion using *Bgl*II and *Xho*I, followed by agarose gel electrophoresis.

The transfection of *P. falciparum* 3D7 was done following the previous report (Sato et al., 2003) with slight modifications. 100 μl infected RBC at approximately 10% ring stage parasitemia was suspended in three volumes of cytomix (van den Hoff et al., 1992) containing 50 μg of plasmid DNA. Total 400 μl of the RBC suspension was electroporated in a 0.2 cm cuvette using Gene Pulser II (Bio-Rad) (0.31 kV, 975 μF). After the transfection, parasites were maintained in the medium supplemented with 5 nM WR99210 as it was described previously (Sato et al., 2003).

2.8. Immunofluorescent studies

Infected erythrocytes and mitochondrial fraction was observed using confocal microscope LSM510 (Zeiss).

Parasites expressing fluorescent protein were incubated for 30 min at 37 °C with MitoTracker Red CM-H_2XRos (Molecular Probes) diluted to 100 nM in culture medium. After the incubation, the culture was once washed with culture medium or AIM medium before microscopy observation.

2.9. Flow cytometry analysis and organelle sorting of transfected parasites

Plasmodium falciparum 3D7 strain expressing GFP was homogenized by nitrogen cavitation method and the crude mitochondrial fraction was prepared according to the procedure described in the previous section. The prepared mitochondrial fraction was analyzed and sorted by EPICS ALTRA (Beckman Coulter). The size of the sorted particles was determined by Flow Cytometry Size calibration Kit (Molecular Probes). Sorted sample were centrifuged and the precipitant was suspended with MSE.

2.10. Detection of organelle by PCR

The primer set to detect apicoplast genome was for the large subunit of rRNA gene, 5′-GAC CTG CAT GAA AGA TG-3′ and 5′-GTA TCG CTT TAA TAG GCG-3′ as it was described previously (Tan et al., 1997). The primer set to detect mitochondria genome was for the subunit I of Complex IV (cytochrome *c* oxidase), 5′-GAC CCA ACA TTT GCA GGA GAT C-3′ and 5′-CAT CAA TGG CAG CAT TAC CTA A-3′. The reaction mixture was prepared with 1 μl of the above mentioned sorted sample (out of final volume 100 μl) or diluted crude mitochondrial fraction, 1× PCR buffer (20 mM Tris–HCl (pH 8.4), 50 mM KCl), 1.25 U *Taq* DNA polymerase (Invitrogen), 1.5 mM $MgCl_2$, 200 μM dNTP and 0.25 μM of each primer in a final volume of 50 μl. The volume of samples was determined not to reach the saturation after the PCR cycle.

The PCR was carried out using the following conditions: pre-heating at 95 °C, 3 min; denaturation at 95 °C, 30 s; annealing at 50 °C, 30 s; elongation at 72 °C, 1 min for 30 cycles followed by incubation at 72 °C for 10 min after the final cycle. For the amplification of mitochondrial genome and apicoplast genome, TEMP CONTROL PC-700 (ASTEC) and GeneAmp® PCR system 9700 (Perkin-Elmer) was used, respectively. Amplified products were then analyzed on a 1% (w/v) agarose gel.

In the experimental procedure, chemicals used were a special grade and were purchased from Wako unless otherwise stated.

3. Results

3.1. The mitochondria and apicoplast co-fractionated by the Percoll density gradient centrifugation

Previously, Fry and Beesley (1991) reported a method to prepare plasmodial mitochondria using a density gradient in 22% (v/v) Percoll formed by centrifugation at 10,000*g* for 5 min. As this method has been successfully used in other laboratories (Wilson et al., 1992; Krungkrai, 1995; Krungkrai et al., 1997), we preliminarily tested if this method is directly applicable to improve the purity of mitochondria prepared by nitrogen cavitation method, which showed higher enzyme activities of mitochondria than those of previous method (Takashima et al., 2001).

We found method reported by Fry and Beesley (1991) is not sufficient to separate mitochondria as g-force was too low and the time was too short (data not shown). Thus, we examined different conditions of Percoll density gradient centrifugation that might improve the current mitochondria sample. To estimate the purity of the obtained mitochondria, activity of mitochondria-specific enzyme, dihydroorotate dehydrogenase (DHOD), which is localized in the inner membrane of the mitochondria was measured. The increase in DHOD-specific activity indicates the enrichment of mitochondria.

We optimized the condition to be 23% (v/v) Percoll centrifuged at 100,000*g* for 1 h at 4 °C using Honduras-1 strain. The gradient was confirmed by the control marker beads in each experiment as it is shown in Fig. 2A. After the Percoll density gradient centrifugation of crude mitochondria sample, prominent brown float and dark brown precipitant were observed (Fig. 2A). The density gradient sample was fractionated and recovery profile of the total DHOD activity after the gradient centrifugation showed two peaks (Fig. 2B). The first peak (fractions 8–10) was sharp and more than twice as high total activity as the broad second peak (fractions 12–16). However, owing to the high amount of proteins recovered, the specific activity in the first peak was not improved. By contrast, the second peak of the total activity showed a significantly higher specific activity; the value of fraction 13 (66.2 ± 27.7 nmol/min/mg protein ($n = 3$)) was about 5 times higher than that of the initial sample (12.4 ± 3.01 nmol/min/mg protein ($n = 3$)). Same results were obtained when the fractionations were performed using 3D7 strain.

To assess the degree of contamination of other cell components, the fractions obtained by the Percoll density gradient centrifugation were analysed by electron microscopy. Fractions 13 and 14, which exhibited the highest DHOD-specific activity, contained a number of mitochondria with double membrane (Fig. 3C and D). Interestingly, another type of multi-membrane-bound organelle was also observed adjacent to the mitochondrion (Fig. 3D). A number of hemozoin particles were found in the crude mitochondria preparation before Percoll density gradient centrifugation (Fig. 3A). Fractions 13 and 14 was virtually free from hemozoin particle (Fig. 3B), although other fractions were prevailed by those bodies (Fig. 3E–G). This suggests that the food vacuole was successfully separated from the mitochondrion by the density gradient centrifugation in 23% (v/v) Percoll.

Since the multi-membrane-bound organelle observed adjacent to the mitochondrion seemed to be the apicoplast,

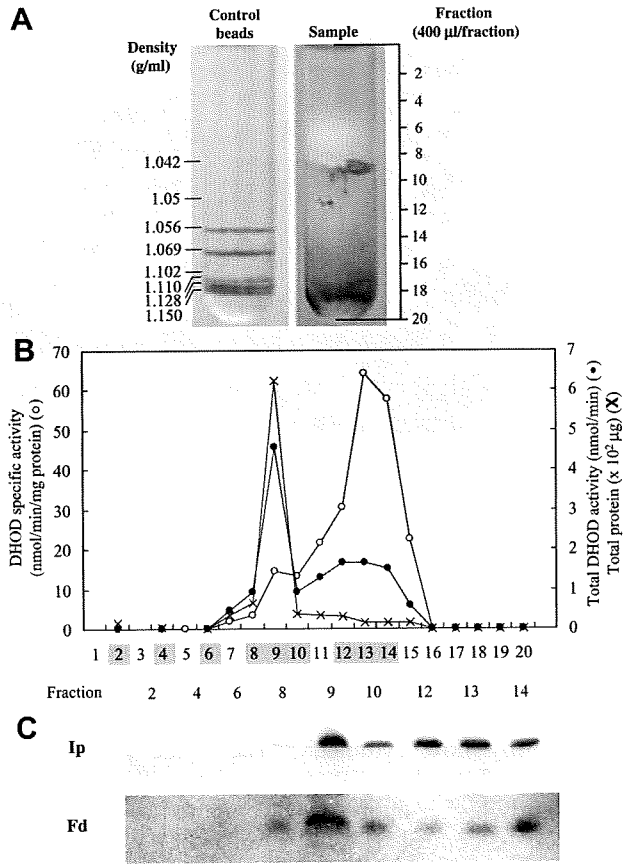

Fig. 2. Percoll density gradient centrifugation. (A) The formation of the gradient was confirmed by beads marker and the density of the control beads were indicated. *P. falciparum* crude mitochondrial fraction was applied to the Percoll density centrifugation forming the brown float and tight brown precipitant. The sample was fractionated from the top to the bottom as indicated. (B) The profile of total protein, DHOD-specific activity and total activity in each fraction of the 23% (v/v) Percoll density gradient centrifugation. The *x*-axis indicates the fraction number and those highlighted were analyzed by the Western blotting. The approximate location of each fraction is briefly indicated in (A). Total protein (X) DHOD total activity (●) and DHOD-specific activity (○). (C) The Western blot analysis of 23% (v/v) Percoll density centrifugation fractions. The localization of mitochondria and apicoplast were determined by using the specific antibodies. Antibody for mitochondria was for succinate dehydrogenase iron–sulfur cluster subunit (Ip) and antibody for apicoplast was for ferredoxin (Fd). eighty microliters of Percoll density fractionation sample was applied each lane.

we probed the fractions made after 23% (v/v) Percoll density gradient centrifugation with the antibody raised against a protein specifically localizing the mitochondrion or the apicoplast. As shown in Fig. 2C, the distribution profile of ferredoxin (Fd), an apicoplast-localizing protein (Vollmer et al., 2001), overlaps that of the iron-sulfer cluster subunit (Ip) of complex II (succinate-ubiquinone reductase), a mitochondrial integral membrane protein (Takeo et al., 2000). This implies even our improved Percoll density gradient centrifugation is not able to separate the mitochondrion from the apicoplast, although it is enough effective to remove the food vacuole or hemozoin particles.

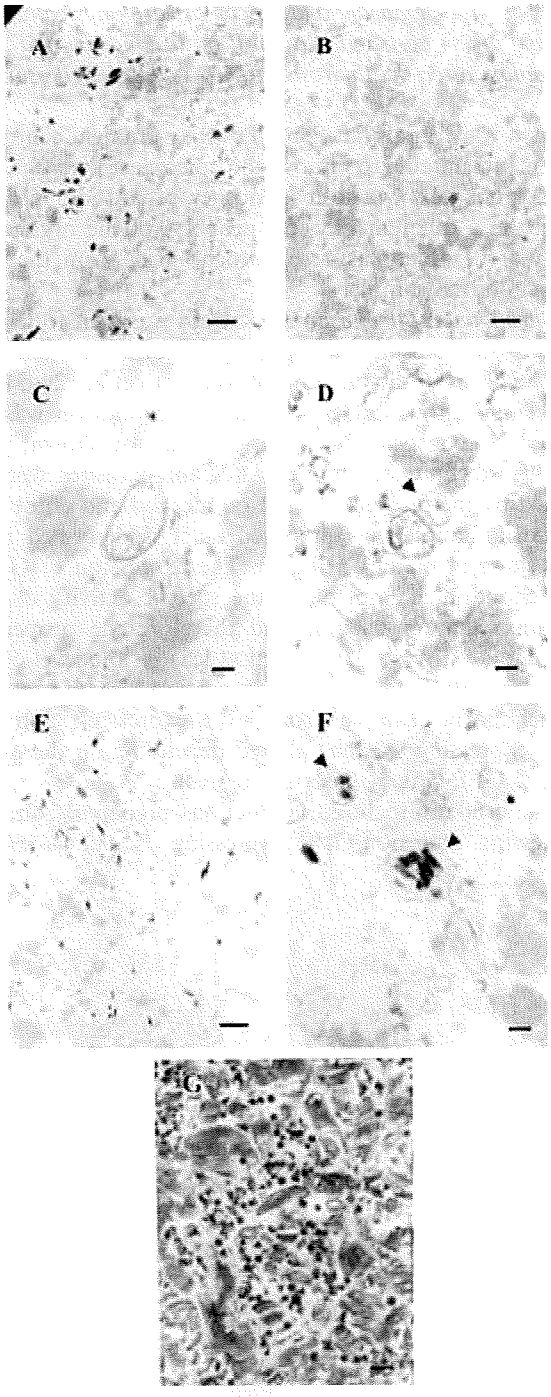

Fig. 3. Electron microscope observation (A) is the crude mitochondria fraction and (B) is the pooled peak fraction of DHOD-specific activity from fraction 13, and 14 after the Percoll density centrifugation (8000×). The dark particles in (A) are significantly reduced in (B), after the Percoll density gradient centrifugation. (C and D) Are observation of the peak DHOD-specific activity at the higher magnification (C; 30,000× and D; 15,000×). The double membrane-bound and multi-membrane-bound structures are indicated by arrows. (E and F) Are the observation of the brown float (fraction 9) at 8000× and 30,000×, respectively. Hemozoin contained in the membrane was observed and from its structure, it is concluded to be a food vacuole. (G) is the tight pellet and the characteristic structure shows it is hemozoin (30,000×). Scale bar; 1 µm for 8000×, 500 nm for 15,000× and 200 nm for 30,000× magnification.

3.2. The mitochondrion and apicoplast are physically bound to each other; co-fractionation of mitochondrion and apicoplast after the fluorescent-activated organelle sorting

As it was found that Percoll density gradient centrifugation is not suitable to remove the apicoplast from the mitochondrion, next we tested another separation technique based on a different physical property of the organelle to recover the apicoplast-free mitochondria from the crude mitochondrial sample.

Plasmodium falciparum 3D7 strain was transfected with a expression plasmid carrying a gene for a GFP derivative that localizes to the mitochondrion (Sato et al., 2003). Specific localization of GFP to the mitochondrion was confirmed by confocal microscope (data not shown) Then, the transfectant and non-transfectant parasites were disrupted by the nitrogen cavitation method and crude mitochondria sample was prepared as it is described in the material and method (Fig. 1). The expression of GFP in mitochondria did not affect the specific activity of mitochondria marker enzyme and therefore the property of mitochondria was not changed at least at the level of electron transfer. In addition, the particle size of the crude mitochondrial sample from GFP-expressing and non-GFP-expressing was not altered depending on the expression of GFP (Fig. 4, inserted figures).

The crude mitochondria fractions prepared from GFP expressing and non-GFP expressing *P. falciparum* was analyzed by flow cytometry. The crude mitochondria preparation from the GFP-expressing transfectant emitted significantly higher fluorescence compared to that of non-transfectant control (Fig. 4A and B). We recovered GFP-positive sample after the fluorescence-activated organelle sorting (FOS) and performed PCR to detect the presence of mitochondria using a specific primers for subunit I of cytochrome *c* oxidase, which is encoded on the mitochondrial DNA. Both the crude sample before FOS and the GFP positive fraction recovered after FOS gave a clear band, confirming the presence of the mitochondrial genomic DNA in these samples (Fig. 5, lanes 1 and 3). In addition, PCR product from apicoplast genomic DNA, large subunit of ribosomal RNA, were also detected (Fig. 5, lanes 2 and 4). This result implies that apicoplast were sorted together with mitochondria by FOS.

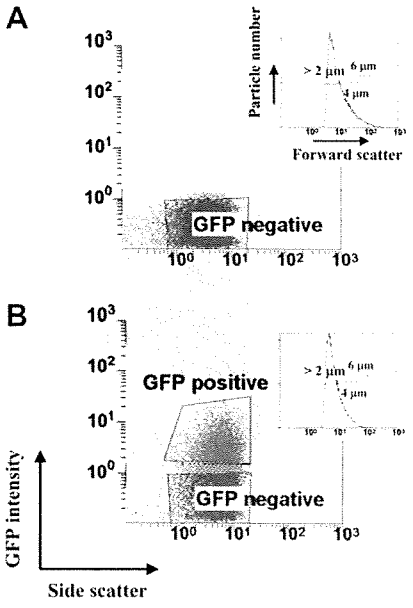

Fig. 4. FOS analysis of crude mitochondria fraction; control and GFP expressing sample. (A) The flow cytometry analysis of the crude mitochondrial fraction from control *P. falciparum* 3D7. The square "GFP negative" indicates the background. (B) The crude mitochondrial fraction prepared from GFP expressing transfectant. The size was determined by the calibration beads. The fraction of the sample expressing significantly high GFP signal were sorted as "GFP positive". The inserted figures show the particle size of the applied crude mitochondria sample.

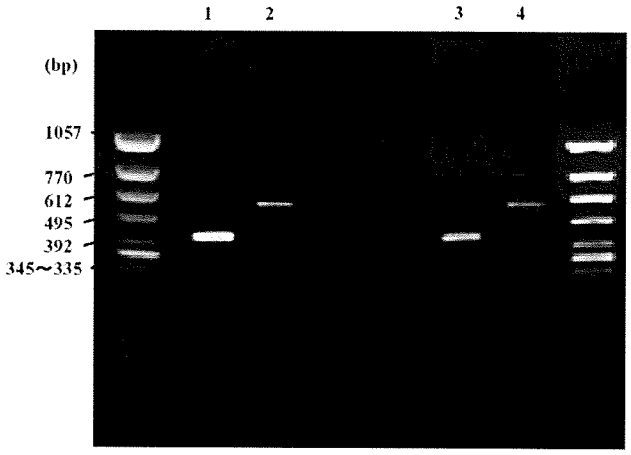

Fig. 5. PCR analysis of mitochondrial fraction and FACS sample. Lanes 1 and 2; crude mitochondria sample. Lane 1 is mitochondria genome-specific primer set and lane 2 is apicoplast genome-specific primer set. Lanes 3 and 4; after the organelle sorting. Lane 3 is mitochondria genome-specific primer set and lane 4 is apicoplast genome-specific primer set. For the detection of mitochondria, the primer set to amplify a part of gene encoding subunit I of cytochrome *c* oxidase was used. For the detection of apicoplast, a part of gene encoding large subunit of ribosomal RNA was used.

4. Discussion

The biochemical study of plasmodial mitochondria has been limited due to the difficulty to prepare sample with high quality and quantity. Previously we have reported the improved mitochondrial preparation from *P. falciparum* using nitrogen cavitation method (Takashima et al., 2001). In this study, we investigated the method to obtain a mitochondrial preparation of better quality by combining nitrogen cavitation with another fractionation method.

Percoll density gradient centrifugation is a well known method to prepare mitochondrial fraction from various organisms including *P. falciparum* and *Plasmodium yoelii* (Fry and Beesley, 1991). The method also has been used for the subcellular fractionation and purification of

mitochondrial enzymes from *Plasmodium* (Krungkrai, 1995, 1997). However, we have found that the purity of the mitochondrial sample prepared by the nitrogen cavitation method could not be improved by the method Fry and Beesley reported (1991). Instead, longer centrifugation with stronger force resulted in a better separation of the mitochondrion (23% (v/v) Percoll, 100,000*g* for 1 h). It is probably because each subcellular structure in the cell was less damaged by nitrogen cavitation in our method than the homogenization with glass-Teflon homogenizer by Fry and Beesley (1991). Indeed, the intact food vacuole containing haemozoin crystals was observed even after our fractionation method (Fig. 3F), and we previously noted that the mitochondrial activity represented by the succinate dehydrogenase was 2 to 3 times higher in of the crude mitochondrial preparation prepared by nitrogen cavitation (Takashima et al., 2001) than those prepared by other conventional methods (Suraveratum et al., 2000).

In this study, the DHOD-specific activity increased about 5 times after the Percoll density gradient centrifugation in the second peak (Fig. 2B), indicating that the contaminants were removed. Indeed, the observation by the electron microscope showed that hemozoin and food vacuole were significantly reduced after the Percoll density gradient centrifugation. Electron microscopic analysis confirmed that the mitochondrion with double membrane was enriched in the fractions forming the second peak (Fig. 3C and D).

Unlike the food vacuole, the apicoplast was not separated from the mitochondrion after the Percoll density gradient centrifugation. It might be because the organelle, by chance, shares the similar density with the mitochondrion. We examined this possibility by a different fractionation method – fluorescence-activated organelle sorting (FOS). Single organelle sorting has been applied to various organelles to determine the characteristics of individual organelle (Böck et al., 1997). The use of fluorescent organelle cytometry attracted scientists' attention to study single mitochondria (Cavelier et al., 2000). In this study, we took the advantage of single organelle sorting to improve the purity of mitochondria sample. After the FOS, the presence of the mitochondrion and the apicoplast genomic DNAs in the GFP positive fraction recovered was confirmed by PCR with target specific primers. This result indicates that applying different mode of fractionation, mitochondria and apicoplast were, again, co-fractionated. Our results strongly suggest that the mitochondrion and the apicoplast of *P. falciparum* are bound to each other.

Up to date, study of mitochondrion and apicoplast of *Plasmodium* has been restricted to the whole cell, and physical interaction between two organelles had not been determined. The extensive genomic information from malaria genome project (Gardner et al., 2002) provided ideas about the putative metabolic pathway in mitochondria and apicoplast in *P. falciparum*. Among those pathways, heme biosynthesis is unique one as the pathway is predicted to begin in the mitochondrion but subsequent reactions are likely taken place in the apicoplast; 5-aminolevulinic acid (ALA), the first intermediate of the pathway, seemed to be synthesized in the mitochondrion via Shemin pathway but converted to porphobilinogen, the next intermediate, in the apicoplast. This peculiarity was experimentally confirmed by localizing ALA synthase and porphobilinogen synthase (ALA dehydratase), respectively (Sato et al., 2004). The parasite may have a requirement to locate these two organelles in a close proximity to facilitate transport of ALA from the mitochondrion to the apicoplast.

The mitochondrion and the apicoplast of *Plasmodium* spp. have been observed in a proximity to each other by electron microscopy and fluorescent microscopy (Aikawa, 1966; Hopkins et al., 1999; Sato et al., 2004; van Dooren et al., 2005), however the strength in the interaction might vary depending on the parasite stage. It is possible that interaction between apicoplast and mitochondrion to be disrupted in the process of mitochondria preparation.

Despite of extensive observations, it is still unknown if there is a significant structure directly connecting these organelles, like tight junction. These organelles can be connected indirectly, e.g., through the cytoskeleton. Both organelles were recovered not only in the fractions forming the second peak with the DHOD activity but also in those forming the first peak after our Percoll centrifugation (Fig. 2). This may suggest that the putative connection between the organelles has a complex structure involving plenty of auxiliary proteins in a physiological state, but can be reduced to a simple, basic structure that is still capable to hold both organelles together.

Acknowledgements

The authors thank late Dr. Masamichi Aikawa for comments on morphological observations by electron microscopy and wish to dedicate this paper to him. The blood and plasma used in this study is a kind donation from Tokyo Metropolitan Red Cross Blood Centre. WR99210, the drug used for the screening of transfected parasites was a kind gift from Jacobus Pharmaceutical Co., Inc. This study was supported by a Grant-in-Aid for scientific research on priority areas and for Creative Scientific Research from the Japanese Ministry of Education, Science, Culture, and Sports (13226015, 13854011, 17209013, 17590368, 18073004 and 18GS0314) and for research on emerging and re-emerging infectious diseases from the Japanese Ministry of Health and Welfare, and by British Medical Research Council.

References

Aikawa, M., 1966. The fine structure of the erythrocytic stages of three avian malarial parasites, *Plasmodium fallax*, *P. lophurae* and *P. cathemerium*. Am. J. Trop. Med. Hyg. 15, 449–471.

Bannister, L.H., Hopkins, J.M., Fowler, R.E., Krishna, S., Mitchell, G.H., 2000. A brief illustrated guide to the ultrastructure of *Plasmodium falciparum* asexual blood stages. Parasitol. Today 16, 427–433.

Böck, G., Steinlein, P., Huber, L.A., 1997. Cell biologists sort things out: analysis and purification of intracellular organelles by flow cytometry. Trends Cell Biol. 7, 499–503.

Bradford, M.M., 1976. A rapid and sensitive method for the quantitation of microgram quantities of protein utilizing the principle of protein–dye binding. Anal. Biochem. 72, 248–254.

Cavelier, L., Johannisson, A., Gyllensten, U., 2000. Analysis of mtDNA copy number and composition of single mitochondrial particles using flow cytometry and PCR. Exp. Cell Res. 259, 79–85.

Feagin, J.E., 1992. The 6-kb element of *Plasmodium falciparum* encodes mitochondrial cytochrome genes. Mol. Biochem. Parasitol. 52, 145–148.

Fry, M., Beesley, J.E., 1991. Mitochondria of mammalian *Plasmodium* spp.. Parasitology 102, 17–26.

Gardner, M.J., Hall, N., Fung, E., White, O., Berriman, M., Hyman, R.W., Carlton, J.M., Pain, A., Nelson, K.E., Bowman, S., Paulsen, I.T., James, K., Eisen, J.A., Rutherford, K., Salzberg, S.L., Craig, A., Kyes, S., Chan, M.S., Nene, V., Shallom, S.J., Suh, B., Peterson, J., Angiuoli, S., Pertea, M., Allen, J., Selengut, J., Haft, D., Mather, M.W., Vaidya, A.B., Martin, D.M., Fairlamb, A.H., Fraunholz, M.J., Roos, D.S., Ralph, S.A., McFadden, G.I., Cummings, L.M., Subramanian, G.M., Mungall, C., Venter, J.C., Carucci, D.J., Hoffman, S.L., Newbold, C., Davis, R.W., Fraser, C.M., Barrell, B., 2002. Genome sequence of the human malaria parasite *Plasmodium falciparum*. Nature 419, 498–511.

Gardner, M.J., Bishop, R., Shah, T., de Villiers, E.P., Carlton, J.M., Hall, N., Ren, Q., Paulsen, I.T., Pain, A., Berriman, M., Wilson, R.J.M., Sato, S., Ralph, S.A., Mann, D.J., Xiong, Z., Shallom, S.J., Weidman, J., Jiang, L., Lynn, J., Weaver, B., Shoaibi, A., Domingo, A.R., Wasawo, D., Crabtree, J., Wortman, J.R., Haas, B., Angiuoli, S.V., Creasy, T.H., Lu, C., Suh, B., Silva, J.C., Utterback, T.R., Feldblyum, T.V., Pertea, M., Allen, J., Nierman, W.C., Taracha, E.L., Salzberg, S.L., White, O.R., Fitzhugh, H.A., Morzaria, S., Venter, J.C., Fraser, C.M., Nene, V., 2005. Genome sequence of *Theileria parva*, a bovine pathogen that transforms lymphocytes. Science 309, 134–137.

Gero, A.M., Brown, G.V., O'Sullivan, W.J., 1984. Pyrimidine de novo synthesis during the life cycle of the intraerythrocytic stage of *Plasmodium falciparum*. J. Parasitol. 70, 536–541.

Greenwood, B.M., Bojang, K., Whitty, C.J., Targett, G.A., 2005. Malaria. Lancet 365, 487–498.

Gutteridge, W.E., Trigg, P.I., 1970. Incorporation of radioactive precursors into DNA and RNA of *Plasmodium knowlesi in vitro*. J. Protozool. 17, 89–96.

Hopkins, J., Fowler, R., Krishna, S., Wilson, I., Mitchell, G., Bannister, L., 1999. The plastid in *Plasmodium falciparum* asexual blood stages: a three-dimensional ultrastructural analysis. Protist 150, 283–295.

Kohler, S., Delwiche, C.F., Denny, P.W., Tilney, L.G., Webster, P., Wilson, R.J.M., Palmer, J.D., Roos, D.S., 1997. A plastid of probable green algal origin in Apicomplexan parasites. Science 275, 1485–1489.

Krungkrai, J., 1995. Purification, characterization and localization of mitochondrial dihydroorotate dehydrogenase in *Plasmodium falciparum*, human malaria parasite. Biochim. Biophys. Acta 1243, 351–360.

Krungkrai, J., Krungkrai, S.R., Suraveratum, N., Prapunwattana, P., 1997. Mitochondrial ubiquinol-cytochrome *c* reductase and cytochrome *c* oxidase: chemotherapeutic targets in malarial parasites. Biochem. Mol. Biol. Int. 42, 1007–1014.

Lambros, C., Vanderberg, J.P., 1979. Synchronization of *Plasmodium falciparum* erythrocytic stages in culture. J. Parasitol. 65, 418–420.

Mi-Ichi, F., Miyadera, H., Kobayashi, T., Takamiya, S., Waki, S., Iwata, S., Shibata, S., Kita, K., 2005. Parasite mitochondria as a target of chemotherapy: inhibitory effect of licochalcone A on the *Plasmodium falciparum* respiratory chain. Ann. N. Y. Acad. Sci. 1056, 46–54.

Prapunwattana, P., O'sullivan, W.J., Yuthavong, Y., 1988. Depression of *Plasmodium falciparum* dihydroorotate dehydrogenase activity in *in vitro* culture by tetracycline. Mol. Biochem. Parasitol. 27, 119–124.

Ralph, S.A., van Dooren, G.G., Waller, R.F., Crawford, M.J., Fraunholz, M.J., Foth, B.J., Tonkin, C.J., Roos, D.S., McFadden, G.I., 2004. Metabolic maps and functions of the *Plasmodium falciparum* apicoplast. Nat. Rev. 2, 203–216.

Roth Jr., E.F., Calvin, M.C., Max-Audit, I., Rosa, J., Rosa, R., 1988. The enzymes of the glycolytic pathway in erythrocytes infected with *Plasmodium falciparum* malaria parasites. Blood 72, 1922–1925.

Sato, S., Rangachari, K., Wilson, R.J.M., 2003. Targeting GFP to the malarial mitochondrion. Mol. Biochem. Parasitol. 130, 155–158.

Sato, S., Clough, B., Coates, L., Wilson, R.J., 2004. Enzymes for heme biosynthesis are found in both the mitochondrion and plastid of the malaria parasite *Plasmodium falciparum*. Protist 155, 117–125.

Sherman, I.W., 1979. Biochemistry of Plasmodium (malaria parasite). Microbiol. Rev. 43, 453–495.

Srivastava, I.K., Rottenberg, H., Vaidya, A.B., 1997. Atovaquone, a broad spectrum antiparasitic drug, collapses mitochondrial membrane potential in a malarial parasite. J. Biol. Chem. 272, 3961–3966.

Srivastava, I.K., Morrisey, J.M., Darrouzet, E., Daldal, F., Vaidya, A.B., 1999. Resistance mutations reveal the atovaquone-binding domain of cytochrome *b* in malaria parasites. Mol. Microbiol. 33, 704–711.

Slomianny, C., Prensier, G., 1986. Application of the serial sectioning and tridimensional reconstruction techniques to the morphological study of the *Plasmodium falciparum* mitochondrion. J. Parasitol. 72, 595–598.

Suraveratum, N., Krungkrai, S.R., Leangaramgul, P., Prapunwattana, P., Krungkrai, J., 2000. Purification and characterization of *Plasmodium falciparum* succinate dehydrogenase. Mol. Biochem. Parasitol. 105, 215–222.

Takashima, E., Takamiya, S., Takeo, S., Mi-ichi, F., Amino, H., Kita, K., 2001. Isolation of mitochondria from *Plasmodium falciparum* showing dihydroorotate dependent respiration. Parasitol. Int. 50, 273–278.

Takeo, S., Kokaze, A., Ng, C.S., Mizuchi, D., Watanabe, J.I., Tanabe, K., Kojima, S., Kita, K., 2000. Succinate dehydrogenase in *Plasmodium falciparum* mitochondria: molecular characterization of the SDHA and SDHB genes for the catalytic subunits, the flavoprotein (Fp) and iron–sulfur (Ip) subunits. Mol. Biochem. Parasitol. 107, 191–205.

Tan, T.M., Nelson, J.S., Ng, H.C., Ting, R.C., Kara, U.A., 1997. Direct PCR amplification and sequence analysis of extrachromosomal Plasmodium DNA from dried blood spots. Acta Trop. 68, 105–114.

Trager, W., Jensen, J.B., 1976. Human malaria parasites in continuous culture. Science 193, 673–675.

Vaidya, A.B., Akella, R., Suplick, K., 1989. Sequences similar to genes for two mitochondrial proteins and portions of ribosomal RNA in tandemly arrayed 6-kilobase-pair DNA of a malarial parasite. Mol. Biochem. Parasitol. 35, 97–107.

van den Hoff, M.J., Moorman, A.F., Lamers, W.H., 1992. Electroporation in 'intracellular' buffer increases cell survival. Nucleic Acids Res. 20, 2902.

van Dooren, G.G., Marti, M., Tonkin, C.J., Stimmler, L.M., Cowman, A.F., McFadden, G.I., 2005. Development of the endoplasmic reticulum, mitochondrion and apicoplast during the asexual life cycle of *Plasmodium falciparum*. Mol. Microbiol. 57, 405–419.

Vincent, R., Nadeau, D., 1983. A micromethod for the quantitation of cellular proteins in Percoll with the Coomassie brilliant blue dye-binding assay. Anal. Biochem. 135, 355–362.

Vollmer, M., Thomsen, N., Wiek, S., Seeber, F., 2001. Apicomplexan parasites possess distinct nuclear-encoded, but apicoplast-localized, plant-type ferredoxin-NADP$^+$ reductase and ferredoxin. J. Biol. Chem. 276, 5483–5490.

Wilson, R.J., Fry, M., Gardner, M.J., Feagin, J.E., Williamson, D.H., 1992. Subcellular fractionation of the two organelle DNAs of malaria parasites. Curr. Genet. 21, 405–408.

Wilson, R.J.M., Denny, P.W., Preiser, P.R., Rangachari, K., Roberts, K., Roy, A., Whyte, A., Strath, M., Moore, D.J., Moore, P.W., Williamson, D.H., 1996. Complete gene map of the plastid-like DNA of the malaria parasite *Plasmodium falciparum*. J. Mol. Biol. 261, 155–172.

Review TRENDS in Parasitology Vol.23 No.5

Parasitology in Japan

Advances in drug discovery and biochemical studies

Kiyoshi Kita[1], Kazuro Shiomi[2] and Satoshi Ōmura[2]

[1] Department of Biomedical Chemistry, Graduate School of Medicine, The University of Tokyo, Tokyo 113-0033, Japan
[2] Kitasato Institute for Life Sciences, Kitasato University and The Kitasato Institute, Minato-ku, Tokyo 108-8641, Japan

Japanese researchers continue to discover new means to combat parasites and make important contributions toward developing tools for global control of parasitic diseases. *Streptomyces avermectinius*, the source of ivermectin, was discovered in Japan in the early 1970s and renewed and vigorous screening of microbial metabolites in recent years has led to the discovery of new antiprotozoals and anthelminthics, including antimalarial drugs. Intensive studies of parasite energy metabolism, such as NADH–fumarate reductase systems and the synthetic pathways of nucleic acids and amino acids, also contribute to the identification of novel and unique drug targets.

Parasitology in Japan: pioneering aspects

Japanese researchers have had a long and successful history in the field of parasitology, perhaps best exemplified by the accomplishments of Kitasato. In establishing a personal and long-term collaboration with Koch and other European researchers and institutes, Kitasato paved the way for numerous compatriots to follow. He also recognized that the public and private sectors had differing but equally important contributions to make in the battle to understand and conquer parasitic diseases. The first man-made chemotherapeutic compound, trypan red, was discovered by Ehrlich and Shiga, who was sent to work alongside Ehrlich from Kitasato's research group in Japan [1]. Trypan red (Figure 1) was effective against trypanosomal infections of mice and its analog, suramin, is still an important drug in human African trypanosomiasis. In Japan, several key infectious diseases, such as malaria and schistosomiasis, have been eliminated and the first successful eradication of filariasis was accomplished in the 1970s by mass administration of the drug diethylcarbamazine [2,3]. Ivermectin, one of the most effective antiparasite drugs, also originated in Japan. This article focuses on recent progress in Japan on novel antiparasite-drug discovery and recent biochemical studies of parasite metabolism that indicate potential new drug targets (Table 1).

Antiprotozoan and metazoan compounds

In Japan, the search for antiparasitic drugs began in earnest in 1922 when Nishi *et al.* produced antimony sodium tartrate (Stibnal®) and showed its effect on *Schistosoma japonicum* [4]. The sodium salt proved less toxic than the previously reported potassium salt. Santonin was isolated from the flower of *Artemisia cina* and used for ascariasis control [5]. It was isolated by Nippon Shinyaku Company Ltd (http://www.nippon-shinyaku.co.jp/) from *Artemisia maritima* in the late 1920s and has been used commercially in Japan since 1940 [6].

New antimetazoans

After World War II, Japan witnessed a flurry of intensive scientific activity and breakthroughs in the fight against parasitic diseases, which resulted in the development of several important antimetazoan-parasite drugs. For example, Yokogawa *et al.* discovered the effectiveness of bithionol in the chemotherapy of paragonimiasis [7] and it was widely used for trematode and cestode infections before praziquantel. Kainic acid, which was isolated from the red alga *Digenea simplex* by Murakami *et al.* [8], was used against some nematode infections as a mixture with santonin. Destomycin A, which is produced by the actinomycete *Streptomyces rimofaciens* and was isolated by Meiji Seika Kaisha Ltd (http://www.meiji.co.jp) [9], is an aminoglycoside that is used for the treatment of nematode infections in the veterinary field.

Isolated by Meiji Seika in the 1990s, PF1022A is a highly effective compound: a cyclic octadepsipeptide nematocide that is produced by the fungus *Rosellinia* spp. [10]. Emodepside, a semisynthetic derivative of PF1022A with a morpholine ring at each of the two D-phenyllactic acids in the para position [11], was later developed by Bayer HealthCare (http://www.bayerhealthcare.com), Meiji Seika and Astellas Pharma Inc. (http://www.astellas.com). Its target was identified as a novel 110 kDa heptahelical transmembrane receptor, named HC-110R, which is similar to mammalian latrophilins [12]. Latrophilins are latrotoxin (black widow spider venom) receptors and G-protein-coupled receptors that are implicated in the regulation of exocytosis. Latrotoxin also binds to HC110-R and causes influx of external Ca^{2+}. Emodepside works as an antagonist to latrotoxin signaling by impairing the influx of Ca^{2+}. It is highly effective against adult stages of the nematodes *Nippostrongylus brasiliensis* and *Strongyloides ratti* in rats and the nematode *Heligmosomoides polygyrus* in mice when used at an oral-dosage range of 1.0–10 mg/kg [11]. It can counteract resistance against the usual classes of anthelmintics and

Corresponding author: Ōmura, S. (omura-s@kitasato.or.jp).
Available online 23 March 2007.

 doi:10.1016/j.pt.2007.03.005

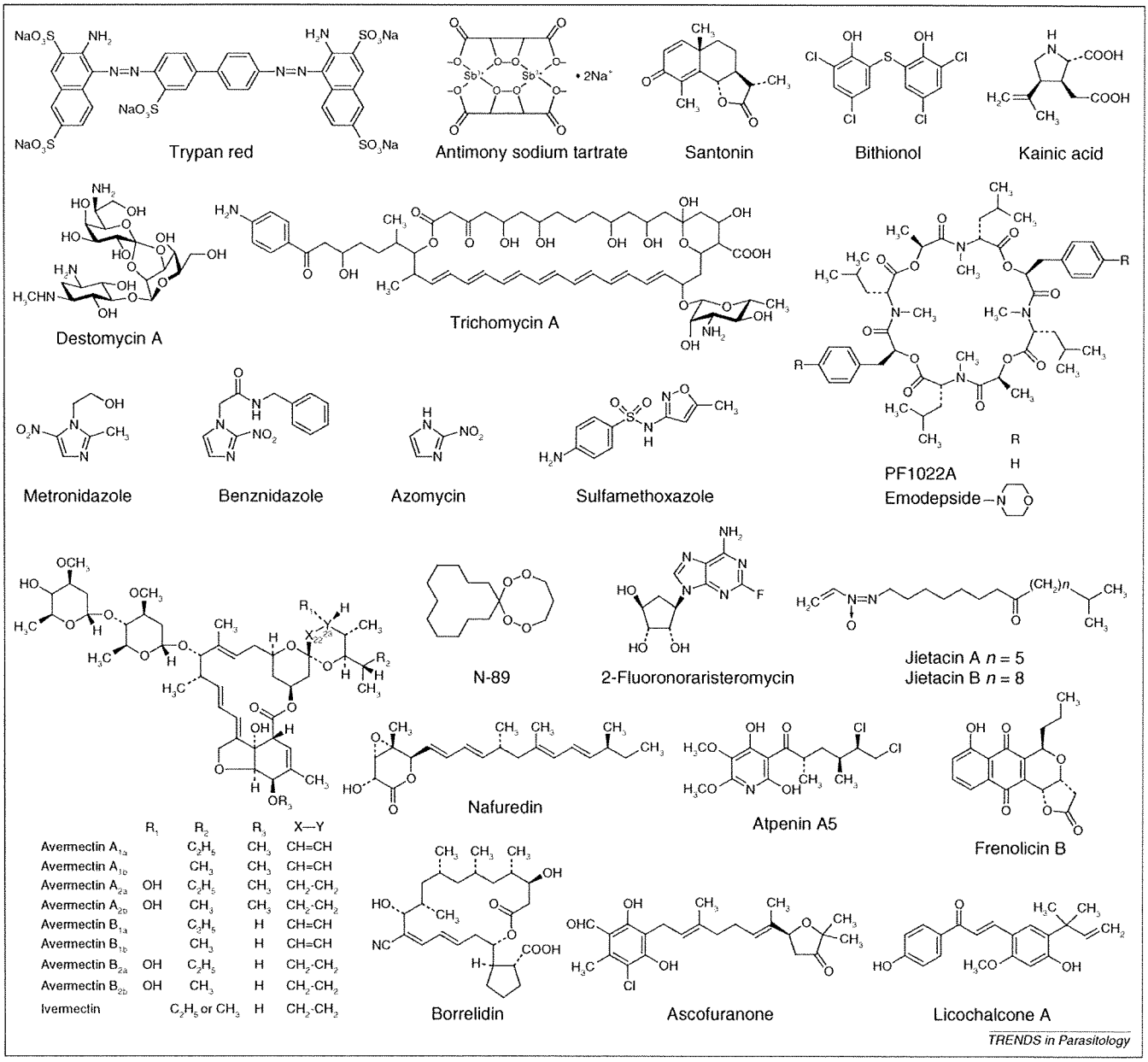

	R_1	R_2	R_3	X—Y
Avermectin A_{1a}		C_2H_5	CH_3	CH=CH
Avermectin A_{1b}		CH_3	CH_3	CH=CH
Avermectin A_{2a}	OH	C_2H_5	CH_3	CH_2-CH_2
Avermectin A_{2b}	OH	CH_3	CH_3	CH_2-CH_2
Avermectin B_{1a}		C_2H_5	H	CH=CH
Avermectin B_{1b}		CH_3	H	CH=CH
Avermectin B_{2a}	OH	C_2H_5	H	CH_2-CH_2
Avermectin B_{2b}	OH	CH_3	H	CH_2-CH_2
Ivermectin		C_2H_5 or CH_3	H	CH_2-CH_2

Figure 1. Structures of antiparasitic compounds that were discovered by Japanese researchers. These compounds are either in current clinical use for parasite diseases or have antiparasitic activity *in vitro* and are good drug candidates. Refs: antimony sodium tartrate [4], ascofuranone [59–62], atpenin A5 [35], avermectins [19–23], azomycin [14,15], benznidazole [71], bithionol [7], borrelidin [38], destomycin A [9], emodepside [11,12], 2-fluoronoraristeromycin [18], frenolicin B [36], ivermectin [24–32], jietacins [33], kainic acid [8], licochalcone A [50], metronidazole [72], N-89 [17], nafuredin [34], PF1022A [10], santonin [5,6], sulfamethoxazole [16], trichomycin A [13], trypan red [1].

was launched in 2005 in Europe as a mixture with praziquantel to eliminate gastrointestinal helminths of cats.

New antiprotozoans

Japan has produced several important antiprotozoan drugs from natural sources. Trichomycin, isolated by Hosoya *et al.*, is used as an antitrichomonal and antifungal antibiotic [13]. It is a mixture of polyene macrolides that are produced by *Streptomyces hachijoensis*. The major component is a 38-membered ring heptaene macrolide, trichomycin A. Nitroimidazole group compounds, such as metronidazole and benznidazole, are derivatives of azomycin, which was isolated from the culture broth of *Streptomyces eurocidicus* by Umezawa *et al.* [14]. After the antitrichomonal activity of azomycin was reported, many such nitroimidazole compounds were then synthesized [15]. Sulfamethoxazole is a sulfa drug that was developed by Shionogi and Company (http://www.shionogi.co.jp) [16] and when mixed with trimethoprim is used as an antibacterial and used for the prevention and treatment of *Pneumocystis carinii*. Recently, several antimalarial candidates have been found by Japanese researchers. Cyclic peroxides with two peroxide groups in the same ring were synthesized by Wataya *et al.* and Nojima *et al.* to be analogous with artemisinin [17]. Among them, N-89 (1,2,6,7-tetraoxaspiro[7.11]nonadecane) showed antimalarial activity comparable to that of artemisinin both *in vitro* and *in vivo* and it cured infection with no parasite

Table 1. Japanese achievements in drug discovery and biochemical studies of parasites

	Year	Research group	Refs
Drug discovery			
Trypan red, the first man-made chemotherapeutic compound	1904	Ehrlich and Shiga	[1]
Antimony sodium tartrate for schistosomiasis	1922	Nishi and colleagues	[4]
Isolation of trichomycin from *Streptomyces hachijoensis*	1952	Hosoya and colleagues	[13]
Isolation of azomycin, the origin of nitroimidazoles	1953	Umezawa and colleagues	[14]
Isolation of kainic acid from *Digenea simplex*	1953	Murakami and colleagues	[8]
Synthesis of sulfamethoxazole	1957	Kano and Ogata	[16]
Bithionol for paragonimiasis	1962	Yokogawa and colleagues	[7]
Isolation of destomycin A from *Streptomyces rimofaciens*	1965	Kondō and colleagues	[9]
Isolation of avermectins from *Streptomyces avermectinius*	1979	Ōmura, Burg, Campbell and colleagues	[20,21]
Isolation of PF1022A, the origin of emodepside	1992	Sasaki and colleagues	[10]
Biochemical studies			
Anerobic respiratory chain of *Ascaris suum*	1984	Oya and colleagues	[39]
Trypanosome alternative oxidase and its specific inhibitor, ascofuranone	1996	Kita and colleagues	[59]
Pyrimidine biosynthetic gene cluster	1999	Aoki and colleagues	[51]
Unsaturated fatty acids essential for *Plasmodium* growth	2000	Mitamura and colleagues	[42]
Stage-specific isoforms of *A. suum* complex II	2003	Kita and colleagues	[41]
Peroxiredoxins in *Plasmodium*	2003	Kawazu and colleagues	[46]
Unique metabolism of sulfur-containing amino acids in *Entamoeba histolytica*	2003	Nozaki and colleagues	[63]

recrudescence or toxicity following oral administration in mice. Work has also indicated that *S*-adenosyl-L-homocysteine hydrolase might be a good target for antimalarial drugs. 2-fluoronoraristeromycin, designed by Kitade *et al.*, showed good selectivity for this enzyme in *Plasmodium falciparum* compared with that in humans [18].

Discovery of avermectins and other antiparasitics

Established by its namesake, The Kitasato Institute (KI: http://www.kitasato.or.jp) has a proud history of antibiotics discovery, including leucomycin (kitasamycin) and mitomycin C. Ivermectin is an endectocide that is active against a diverse range of nematodes, insects and arachnids and has its origins in the institute [19]. Ivermectin is now recognized by many as one of the most important drugs in human and animal health of the past century. In 1973, researchers at the KI started to screen nematocidal antibiotics in collaboration with Merck, Sharpe and Dohme Research Laboratories (MSD: http://www.msd.com). The Kitasato group isolated cultures from soil samples and undertook *in vitro* evaluation of the fermentation broths. In the MSD laboratories, promising cultures were screened using a novel model of helminth infection – mice infected with the nematode *Nematospiroides dubius*. The broth of strain MA-4680 exhibited potent anthelmintic activity [20]. This strain originated in a soil sample collected at Kawana, Shizuoka prefecture [21] and was classified as a new species of actinomycetes and named *Streptomyces avermectinius* (formerly *Streptomyces avermitilis*) [22]. Eight active components were isolated from the broth and named avermectins A_{1a}–B_{2b}. Compounds of the B series, which have a 5-hydroxy group, are markedly more active than those of the A series, which have a 5-methoxy group. Reduction of the 22,23-olefin of the most active avermectins B_{1a} and B_{1b} improved both the activity spectrum and the safety and the resulting 22,23-dihydro B_1 complex (as a mixture of 80% B_{1a} and 20% B_{1b}) was marketed as a veterinary drug under the generic and nonproprietary name ivermectin in 1981 [23].

Ivermectin is used for the control of economically important nematodes that infect the gastrointestinal tract, lungs and kidneys, in addition to other nematodes of livestock such as *Thelazia* and *Parafilaria*. It is also used against several arthropod parasites, including grubs, lice, mites and screw worms [24]. In companion animals, it provides good control of *Dirofilaria immitis*. Ivermectin was later found to be safe and highly effective in controlling some nematode infections in humans. Of greatest importance is that it proved highly efficacious against microfilariae of *Onchocerca volvulus*, which causes river blindness. Unique, pioneering and multifaceted public–private partnerships (PPPs) were established and eventually incorporated several United Nations agencies (http://www.un.org) and nongovernmental organizations. These PPPs enabled the donation of ivermectin (under the brand name Mectizan®) and led to a model for a highly successful mass drug administration (MDA) program that should culminate in the elimination of onchocerciasis in the endemic areas of Africa and the Americas [25]. Ivermectin is a remarkably safe and effective broad-spectrum drug. Side effects, when they do occur, are minimal and tolerable, usually resulting from inflammatory and immune defenses that are triggered by immobilized or dead microfilariae [26]. Therefore, ivermectin can be administered by nonmedical individuals after a modicum of training and can be used in MDA programs that are run by affected communities themselves. Although ivermectin is also effective against *Loa loa* [26], a few severe adverse events have occurred in individuals with high levels of *L. loa* microfilariae that have been treated with ivermectin [27]. Recently, ivermectin has also become an invaluable tool for a global elimination initiative against lymphatic filariasis, a disease that is caused by infection with *Wuchereria bancrofti* and *Brugia malayi* [26]. This means that the drug will be available free of charge in order to rid the world of two devastating diseases and to improve the lives of hundreds of millions of people. Ivermectin has now been found to be the most useful agent for strongyloidiasis [28]. In addition to the control of nematode infections, ivermectin also shows efficacy against human scabies, which is caused by infection with the ectoparasitic mite *Sarcoptes scabiei* [29].

Avermectin targets a parasite-specific glutamate-gated chloride channel [30], which it activates to cause neurological disruption of the parasite. Although avermectins also bind to γ-aminobutyric acid-gated and glycine-gated chloride channels in mammals, their affinity for invertebrate receptors is ~100-times higher. Mice that have the P-glycoprotein gene knocked out showed increased sensitivity to ivermectin [31]. This result established an important role for P-glycoprotein in the maintenance of the blood–brain barrier and indicated that the safety of ivermectin is because of the blood–brain barrier, in addition to the low affinity of the receptors.

In 2003, the Kitasato group elucidated the complete genetic sequence of *S. avermectinius* [32]. The genome is the largest bacterial genome yet sequenced (9026 kb) and encodes ≥7574 potential open reading frames. Analysis identified the gene cluster that is involved in secondary-metabolite production and sheds light on the biology of microbial secondary-metabolite synthesis at the genetic level, thus offering the prospect of creating some new metabolites.

After the discovery of avermectin, the Kitasato group isolated jietacins A and B from the culture broth of *Streptomyces* spp. using the pine wood nematode, *Bursaphelenchus lignicolus* [33]. Jietacins show a ~10-times higher nematocidal activity than avermectin B_{1a} against *B. lignicolus in vitro*. Nafuredin, produced by the fungus *Aspergillus niger*, was found during screening for an NADH–fumarate reductase inhibitor [34]. It inhibits helminth electron transport enzyme complex I and shows anthelmintic activity against *Haemonchus contortus* in sheep (see later). Atpenin A5 was discovered during the same screening and is the most potent complex II inhibitor. It might, therefore, be a useful tool for clarifying the biochemical and structural properties of complex II [35]. In the case of antiprotozoan compounds, frenolicin B, which is produced by *Streptomyces roseofulvus*, has potent anticoccidial activity in *Eimeria tenella* infection in chicks [36].

Building on the increased global awareness that the public and private sectors need to work together if the major communicable diseases are to be overcome, a PPP that includes leading Japanese pharmaceutical companies, the Japanese Ministry of Health, Labour and Welfare, and the World Health Organization was established in 1999 to discover new antimalarials [37] and is collectively known as the JPMW project. A screening center was established at the KI in which evaluation of antimalarial activity of compounds is carried out both *in vitro* and using the rodent malaria model. These compounds come from two sources: those donated from the chemical libraries of 14 Japanese companies and natural products from the KI. More than 30 000 compounds have been screened since 2000 and one compound, borrelidin, shows excellent antimalarial activity in both *in vitro* chloroquine (CQ)-susceptible and CQ-resistant *P. falciparum* models [38]. It also has antimalarial activity against rodent malaria. The effective dose is lower than that required for artemether, artesunate and CQ itself. The 90% effective dose (ED_{90}) values of orally-administered borrelidin, artemether, artesunate and CQ against CQ-resistant *P. yoelii*-infected mice were 1.1, 40, >50 and >100 mg/kg, respectively [38].

Elucidation of biochemical targets in protozoan and metazoan parasites

Parasites have developed a range of physiological functions that are necessary for their survival within the specialized environment of the host and studies of these parasitic adaptations have provided interesting biological discoveries [39]. Recent advances in biochemical and molecular biological approaches have provided new knowledge and led to many breakthroughs in the field of biological evolution and parasite diversity, with the novel understanding of unique aspects of parasite metabolism heralding promising targets for chemotherapy.

The anerobic respiratory chain of mitochondria in helminths

Recent research by Kita *et al.* on the respiratory chain of the parasitic helminth *A. suum* has shown that the mitochondrial NADH–fumarate reductase system (Figure 2) has an important role in the anerobic energy metabolism of adult parasites, in addition to unique features of the developmental changes that occur during their life cycle [39]. In this system, the reducing equivalent of NADH is transferred to the low-potential rhodoquinone (RQ) by the NADH–RQ reductase complex (complex I). This pathway ends with the production of succinate by the rhodoquinol–fumarate reductase activity of complex II [succinate–ubiquinone (UQ) reductase in aerobic respiration]. Electron transfer from NADH to fumarate is coupled to site I phosphorylation of complex I by generation of a protonmotive force. The difference in redox potential between the NAD^+–NADH couple ($Em' = -320$ mV) and the fumarate–succinate couple ($Em' = +30$ mV) is sufficiently high to drive ATP synthesis. The anerobic NADH–fumarate reductase system is found not only in nematodes but also in bacteria and many other parasites.

An anthelmintic compound, nafuredin, selectively inhibits helminth complex I at nanomolar concentrations [34]. Kinetic analysis showed that the inhibition by nafuredin is competitive against an exogenous RQ. These findings, coupled with the fact that helminth complex I uses both RQ and UQ as an electron acceptor, indicate that the structural features of the quinone reduction site of helminth complex I might differ from that of mammalian complex I. In fact, the inhibitory mechanism of quinazolines was competitive against RQ and partially competitive against UQ [40].

Amino *et al.* have demonstrated that *A. suum* mitochondria express stage-specific isoforms of complex II: the flavoprotein subunit and the small subunit of cytochrome *b* of the larval complex II differ from those of the adult enzyme, although two complex IIs share a common iron–sulfur cluster subunit [41]. Enzymatic assays indicated that *A. suum* complex IIs have different properties compared with complex IIs of mammalian hosts and that the larval complex II is able to function as a rhodoquinol–fumarate reductase. As mentioned earlier, the most potent inhibitor of complex II, atpenin A5, was found during screening of inhibitors for the *A. suum* complex II [35]. Osanai *et al.* obtained a crystal of adult complex II and an analysis of parasite-specific factors in the enzyme complex is now in progress.

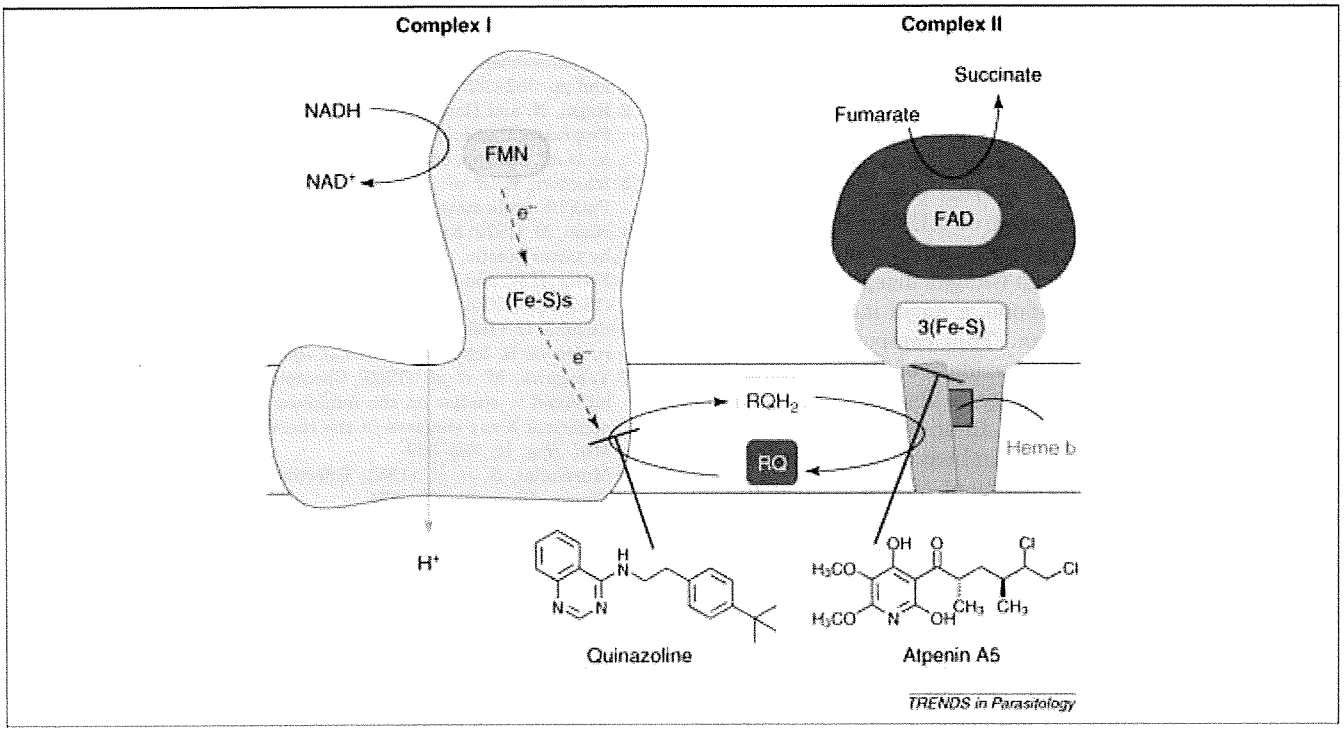

Figure 2. NADH–fumarate reductase system in *Ascaris suum* mitochondria. The respiratory inhibitors quinazoline [40] and atpenin A5 [35] inhibit *A. suum* complex I and complex II, respectively. Nafuredin (see Figure 1) also inhibits *A. suum* complex I [34]. Figure by K. Sakamoto, University of Tokyo.

Unique *Plasmodium* enzymes

P. falciparum is the causative agent for the most severe form of malaria in humans. Because clinical symptoms and complex pathogenesis are exclusively associated with the asexual multiplication of this parasite in erythrocytes, Mitamura and colleagues have focused on intra-erythrocytic proliferation of *P. falciparum* and lipid metabolism and trafficking in parasitized erythrocytes [42]. They found that limited combinations of saturated and unsaturated free fatty acids (the best combination of which is palmitic and oleic acids) are essential serum factors that are required for parasite growth to ensure complete intra-erythrocytic development and cell cycle progression [42]. This finding showed that scavenging free fatty acids from host serum is crucial for the survival of intra-erythrocytic *Plasmodium* parasites. Furthermore, Mitamura and colleagues have shown genetic evidence that *P. falciparum* diacylglycerol acyltransferase 1, a principal enzyme for triacylglycerol biosynthesis, seems to have a crucial role in the intra-erythrocytic proliferation of the parasite [43]. Their work on lipid metabolism and trafficking in *P. falciparum* has attracted attention with respect to both basic biology and its potential application for malaria chemotherapy [44].

Because the parasites do not possess catalase or glutathione peroxidase, the bulk of peroxide-reducing capacity in the cell seems to be provided by peroxiredoxins (Prx) [45]. Kawazu and his group reported that disruption of the gene that encodes the cytosolic 2-Cys Prx (PfTPx-1) in *P. falciparum* renders parasites hypersensitive to reactive oxygen and nitrogen species [46]. They also showed that the other cytosolic Prx (Pf1-Cys-Prx) might help to protect the parasite against oxidative stress that results from hemoglobin metabolism [47]. These findings indicate that parasites use the Prx proteins on different occasions for management of intracellular oxidative stresses during their intra-erythrocytic development [48]. How the parasite regulates proper expression of the antioxidant proteins under different physiological situations is a matter of great interest.

Differences between the mitochondria of malaria parasites and those of the host are also expected to indicate potential targets for chemotherapy. Using active mitochondria that have been isolated from *P. falciparum* [49], Miichi *et al.* investigated the licochalcone A-inhibited bc_1 complex (ubiquinol–cytochrome *c* reductase), in addition to complex II (succinate–ubiquinone reductase) of *P. falciparum* mitochondria [50]. Because the properties of the *P. falciparum* bc_1 complex are different from those of the mammalian host and are a target of atovaquone, chalcones are promising candidates for new antimalarial drugs.

Targets in trypanosomes and ameba

Nara and coworkers reported a novel, polycistronic pyrimidine-biosynthetic (*pyr*) cluster that contains five genes (*pyr1*, *pyr3*, *pyr6–5*, *pyr2* and *pyr4*) and encode all six enzymes that are involved in pyrimidine biosynthesis in *Trypanosoma cruzi* and *Leishmania* spp. [51]. Although most eukaryotes carry *pyr5–6*, kinetoplastids possess the conversely fused *pyr6–5*. This biosynthesis pathway is essential for protozoan survival [52,53]. In particular, the *pyr4*- and *pyr6*-encoded enzymes are promising drug targets because they differ biochemically from those of their mammalian-host counterparts, probably because these genes have been horizontally acquired [53–55]. Phylogenetic studies of the kinetoplastid *pyr6–5* indicated that